Numerical investigation on corner singularities in cracked plates using the G-theta method with an adapted theta field

Minh Ngoc Vu, Samuel Geniaut, Patrick Massin, Jean-Jacques Marigo

Numerical investigation on corner singularities in cracked plates using the G-theta method with an adapted θ field

M.N. Vu[a,1] , **S. Geniaut**[a,b,*], **P. Massin**[a], **J.J. Marigo**[c]

[a] LaMSID-Laboratoire de Mécanique des Structures Industrielles Durables (EDF/CNRS/CEA), Clamart, France
[b] Département AMA - EDF R&D, Clamart, France
[c] Laboratoire de Mécanique des Solides, Ecole Polytechnique, Palaiseau, France

* Corresponding author: Tel : +33 1 47 65 59 71, Email : samuel.geniaut@edf.fr

Abstract

G-theta method with appropriated virtual crack extension (**θ** field) is proposed for the accurate evaluation of energy release rate along a crack edge which is non-orthogonal to the free surface. This method is implemented in the framework of finite element procedure as well as extended finite element one. This numerical procedure is then applied to investigate the corner singularities in cracked plates. The superposition of numerical solution to asymptotic solution within the boundary layer of crack front allows showing the dependence of vertex singularity to plate thickness.

Keywords: G-theta, θ field, corner singularity, cracked plate, critical angle

1 Introduction

Accurate evaluation of stress intensity factor or of energy release rate is an important key for 3D modeling of surface crack growth. Due to the complexity of such problems, exact solutions are not available and numerical methods impose naturally. The finite element method has become the most commonly used numerical procedure to obtain crack surface evolution. Stress intensity factors can be determined from local stresses or displacement fields around the crack tip. The quarter-point technique is usually used to ensure the square-root stress singularity in the neighborhood of the crack front [2]. This technique can be combined with techniques such as J-integral [45], M-integral [50], G-thetha method [13] and many others, which allows obtaining by post-processing the relevant parameters of fracture mechanics. Alternative finite element approaches used with hybrid elements [1], or enriched

[1] Now at ANDRA – R&D Division, 1-7 rue Jean Monnet, F-92298 Chatenay-Malabry, France

element methods [7, 23] directly include stress singularity factors as unknowns in the displacement fields.

G-theta method was proposed by Destuynder et al. [13] for calculating the energy release rate and stress intensity factors. This method is based on domain integrals and Lagrangian derivation of the potential energy, with respect to a virtual crack extension velocity field ($\boldsymbol{\theta}$ field). G-theta procedure, available in Code_Aster software [17], is used as a post-processing of FEM or XFEM calculations. The $\boldsymbol{\theta}$ field definition uses the local basis at the crack front which is normal to the crack front and tangent to the crack surface. Inside the solid, its direction is orthogonal to the crack front, given by the projection on the crack front, which is the common practice [25, 26, 27]. For a through crack surface, the θ field, at the terminal point of the front edge, is modified in the present paper to be tangent to the free surface. In case the crack front intersects non-orthogonally the free surface, the $\boldsymbol{\theta}$ field changes of direction between the terminal point and adjacent interior nodes on the crack front, more or less rapidly. In case of rapid change, numerical instabilities and inaccuracies are observed during the propagation of such cracks. This paper aims firstly at introducing automatically a modified θ field to circumvent the inconvenience of standard normal θ fields. The crack front of a through crack surface is divided into two or three parts: an internal part and modified parts connected to terminal points on the free surface, at a maximum of two. On the internal part, a θ field normal to the crack front is used. On the modified parts, the direction of the θ field varies continuously from the direction at the terminal point, where it is tangent to the crack surface and the free surface, and the one of the internal part where it is normal to the crack front. The implementation of the modified $\boldsymbol{\theta}$ field is also an opportunity to show some interesting properties of the G-theta method such as its independence with respect to $\boldsymbol{\theta}$ direction and integral domain size, which are not observed with a normal $\boldsymbol{\theta}$ field in case of through cracks. Besides, the proposed modified θ field allows determining correctly the energy release rate in the boundary layer region close to the free surface. This result is used then to investigate numerically the corner singularity in a cracked plate.

In three dimensional fracture mechanics, the concept of stress intensity factor is based on the implicit assumption that the crack front is continuous and infinite. This is not the case at a terminal point where the crack front intersects a free surface. As a matter of fact, the stress singularity order changes in the vicinity of a corner point, its value depending on Poisson's ratio and on the intersection angle between the crack front and the free surface [4, 14, 22, 44]. Several techniques were developed to determine the vertex singularity, which can be classified into two categories: global and local approaches. The global approach consists in determining directly the stress singularity exponent from the resolution of a linear elastic problem containing corner singularity such as: semi-analytical method [5], finite different

method [6], singular integral equation method [24, 34, 35, 39, 40, 46], eigenvalue problem [3, 4, 14, 16, 21, 22, 49]. The local approach is based on the logarithmic regression of stress or displacement fields in the vicinity of the crack tip [31, 32, 38, 47] or of stress intensity factors in the boundary layer region close to the free surface [41, 42]. Using a semi-analytical method, the vertex singularity of a quarter-infinite crack is calculated firstly by Benthem [5]. In an attempt to develop a more general method, Bazant and Estenssoro [4] turned to the finite element method and showed the stress singularity exponent is solution to a quadratic eigenvalue problem. Afterwards, several studies have been devoted to improve the numerical scheme in terms of convergence speed [16, 21 35, 43, 49]. However, the global approach deals only with vertex singularity point in a half-space. Extracting the stress singularity exponent from the stress or displacement field, by using the logarithmic regression, is usually used to evaluate corner singularity in cracked middle tension specimens [30, 38, 47, 48]. This technique is highly sensitive to element size around the crack tip. Moreover, the result obtained with the logarithmic regression of displacements sometime depends on the polar angle of the cylindrical local frame centered at the crack tip. Based on the asymptotic expression of the energy release rate in the neighborhood of a corner point singularity derived by Leguillon [36], Leguillon and Sanchez-Palencia [37], a technique is proposed in this work to investigate the vertex singularity in a cracked plate. The numerical result of the energy release rate obtained with the modified θ field is superposed to the asymptotic formulation within the boundary layer region on the crack front close to the free surface. The results bring out the influence of plate thickness on stress singularity exponent and critical angle.

The numerical development related to the introduction of a modified θ field in the G-theta method have been implemented in Code_Aster [17], an industrial and open source finite element code developed by EDF R&D. This code is also used for the numerical investigation of the corner singularity carried out in Section 3.

2 G-theta method

2.1 G-theta formulation

We consider a reference body Ω containing a crack Γ with traction-free surface. Destuynder et al. [13] gave the variation of the potential energy induced by an infinitesimal perturbation applied on the reference geometry Ω on which the solution (σ, $\underline{\boldsymbol{u}}$) is known. The geometrical perturbation transforms a point M of the cracked body Ω into a point M_η such that: $M_\eta = M + \eta.\theta(M)$. In the framework of thermo-elasticity and in the absence of body forces, the global energy release rate associated to the virtual crack extension field θ is given by:

$$\mathrm{G}(\boldsymbol{\theta}) = \int_{\Omega} \left(\boldsymbol{\sigma} : (\nabla \boldsymbol{u} \nabla \boldsymbol{\theta}) - \psi \nabla . \boldsymbol{\theta} - \frac{\partial \psi}{\partial T} (\nabla T . \boldsymbol{\theta}) \right) d\Omega \tag{1}$$

where, σ is the Cauchy stress tensor, u the displacement filed, T the temperature field, ψ the energy density. The virtual crack extension field $\boldsymbol{\theta}$ must be tangent to the crack surface at the crack front and must be tangent to the boundaries of the body (i.e $\boldsymbol{\theta}.\boldsymbol{n} = 0$ on $\partial\Omega$, where $\boldsymbol{n}$ is normal to $\partial\Omega$). Based on a Lagrangian approach of the potential energy derivative, the local energy release rate $G(s)$ along the crack front Γ is obtained from the following equation [13]:

$$\int_{\Gamma} G(s) \boldsymbol{\theta}(s) . \boldsymbol{m}(s) = \mathrm{G}(\boldsymbol{\theta}) \tag{2}$$

with $\boldsymbol{m}(s)$ the vector tangent to the crack surface and normal to crack front along the curvilinear abscissa s.

The numerical discretization of Eq. (2) is performed with a decomposition of $G(s)$ on a basis $p_j(s)$ ($1 \leq j \leq N$). Supposing G_j the components of $G(s)$ in this basis, we obtain:

$$G(s) = \sum_{j=1}^{N} G_j p_j(s) \tag{3}$$

A set of function tests for the field $\boldsymbol{\theta}$ such as: $\Theta = \{\boldsymbol{\theta}_i$ where $\boldsymbol{\theta}_i . \boldsymbol{n} = 0$ on $\partial\Omega\}$ ($1 \leq i \leq M$) is then chosen. Substituting (3) into (2) leads to:

$$\int_{\Gamma} \left(\sum_{j=1}^{N} G_j p_j(s) \right) \boldsymbol{\theta}(s) . \boldsymbol{m}(s) = \mathrm{G}(\boldsymbol{\theta}) \qquad \forall \boldsymbol{\theta} \subset \Theta \tag{4}$$

Furthermore,

$$\sum_{j=1}^{N} G_j \left(\int_{\Gamma} p_j(s) \boldsymbol{\theta}_i(s) . \boldsymbol{m}(s) \right) = \mathrm{G}(\boldsymbol{\theta}_i) \qquad \forall i \in [1, M] \tag{5}$$

Therefore, the components G_j constitute N unknowns of the linear system of M equations:

$$\sum_{j=1}^{N} A_{ij} G_j = \mathrm{B}_i \qquad i \in 1, M \tag{6}$$

where:

$$A_{ij} = \int_{\Gamma} p_j(s) \boldsymbol{\theta}_i(s) . \boldsymbol{m}(s) ds \ , \qquad \mathrm{B}_i = \mathrm{G}(\boldsymbol{\theta}_i) \tag{7}$$

In order to avoid the inaccuracy of the results near the crack front where $\nabla \mathbf{u}$ is singular, it is interesting from a numerical point of view to introduce a constant $\boldsymbol{\theta}$ field in the vicinity of Γ

in Eq. (1). In practice, we consider two toroid surfaces surrounding the crack front Γ of radius R_{ext}, R_{int} ($R_{int} < R_{ext}$) within the solid (Fig. 1a). At each point of curvilinear abscissa s on Γ, the θ field $\boldsymbol{\theta}(s)$ is built in the plane perpendicular to the crack front Γ as follows (Fig. 1b):

$$\begin{aligned} &\boldsymbol{\theta} = \boldsymbol{\theta}(s) && \text{for } 0 \le r(s) < R_{int}(s) \\ &\boldsymbol{\theta} = \frac{R_{ext}(s) - r(s)}{R_{ext}(s) - R_{int}(s)}\boldsymbol{\theta}(s) && \text{for } R_{int}(s) \le r(s) \le R_{ext}(s) \\ &\boldsymbol{\theta} = 0 && \text{for } r(s) > R_{ext}(s) \end{aligned} \qquad (8)$$

The introduction of the θ field, the choice of basis p_j for G(s) and the numerical implementation for the resolution of Eq. (6) in Aster_Code are presented in detail by Geniaut [19]. The function test field θ is introduced such that θ is normal to the crack front verifying: $\boldsymbol{\theta}.\boldsymbol{m} = 1$ (Fig. 2a). Moreover, the θ field must be known at every points of the cracked body in order to calculate the global energy release rate G(θ) in Eq.(1). Therefore, it is necessary to extend the θ field to each node of the mesh from the known vectors on the crack front. The projection algorithm of a node on the crack front in the direction of the θ field decomposes in two steps: searching the segment on the discretized crack front containing the projection point, and then locating the projection point on this segment. For the normal θ field, each node is projected orthogonally to the crack font and the θ field direction assigned to this node is the one of its projection point on the crack front [9, 20]. The θ field direction at the projection point on the crack front is then computed from the ones of the extremity nodes of the segment on which the projection point is located [10, 11, 12]. This choice allows integrating analytically A_{ij} in Eq. (7). However, such θ field does not give an accurate energy release rate when the crack front intersects non-orthogonally the free surface. In this case it can be shown that on the free surface the θ field must remain tangent to the free surface and that the change of θ direction must be smooth between the corner point and the adjacent internal points (Fig. 2b). To avoid this source of error, a modified θ field is introduced to treat this situation in the next section.

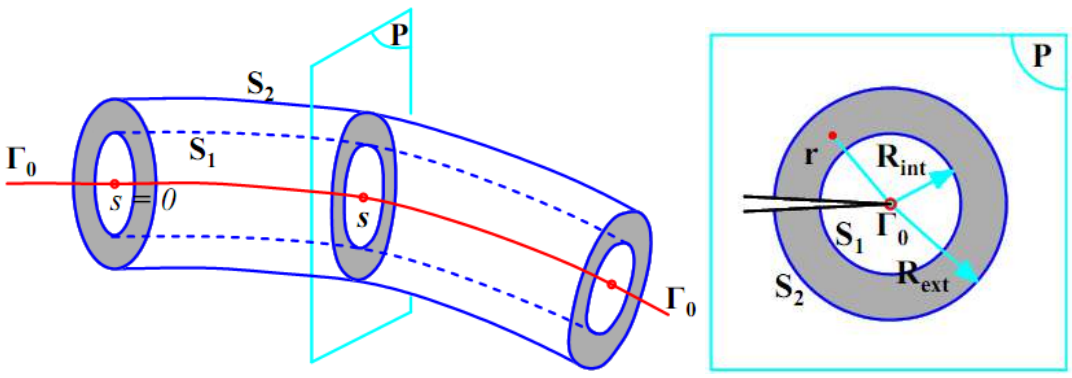

Fig. 1 : θ field construction in tridimensional problem.

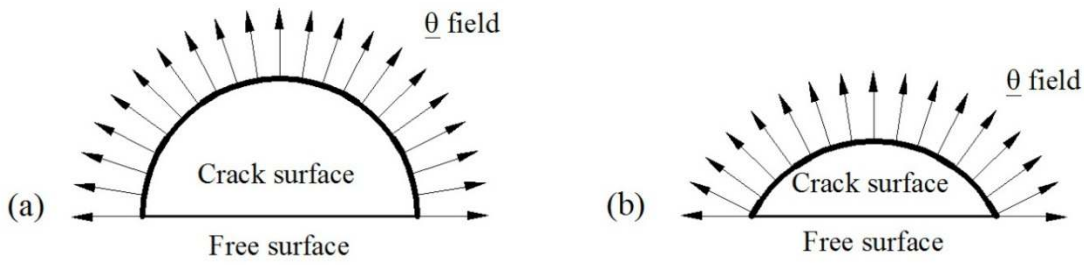

Fig. 2 : θ field on the crack front of through crack surface: (a) orthogonal crack front, (b) non-orthogonal crack front.

2.2 Modified θ fields

In case of through crack surface with non-orthogonal crack fronts to free surfaces, a modified **θ** field is proposed to improve the accuracy of the numerical result. With respect to the previous version of Aster_Code [17], the **θ** field is tangent to the free surface at the through point and normal to the crack front inside the solid. In the intermediary portion of length L_m, a linear variation of direction between the through point and the internal points is chosen (Fig. 3). The length L_m is given by the user: it must be lower than half the crack front length $0.5L$ and larger than L_{min} (Fig. 4). The value of L_{min} can be determined analytically in some cases such as straight crack fronts, part-circular cracks and other simple geometric profiles.

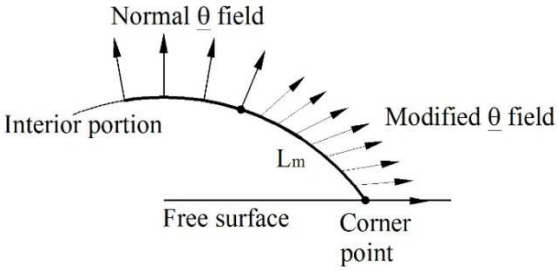

Fig. 3 : Modified θ field on the crack front of breaking crack surface.

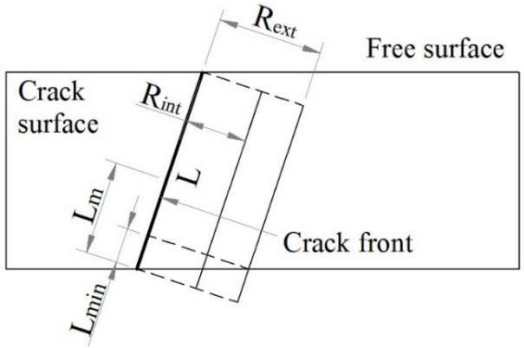

Fig. 4 : Length L_m on which the **θ** field is modified for a non-orthogonal crack front to the free surface.

Such a modified **θ** field leads to numerical evaluation of the integration terms A_{ij} in Eq. (7). In order to have the directions of the modified θ field everywhere in the solid an extension of

this field within the solid is used based on non orthogonal projections on the crack front along the θ directions defined on it. In order to have its modulus we keep on using the distance to the crack front. The algorithm detail of this projection as well as numerical resolution of Eq. (2) is expressed in [9].

To show the improvement on the numerical results obtained with this modified $\boldsymbol{\theta}$ field compared to the classical normal one, a cracked plate under uniform applied stress σ (Mode I) is considered (Fig. 5). All results presented in this section, unless otherwise stated, refer to σ = 1 MPa. The material is assumed to be homogeneous and isotropic with an elastic modulus E =210 GPa and a Poisson's ratio ν = 0.3. The geometry parameters defined in Fig. 5 are $a = b$, $H = l = 10a$. A value of a = 0.5 m was chosen to obtain our results. The crack front has an angular point at its middle and two through points on the free surface. The crack surface is located at the half height of plate H.

Exploiting the symmetry in geometry and loading, only one-fourth of the specimen was modeled in the finite-element analysis. Fig. 6 illustrates the finite element mesh used for modeling. A twenty-node isoparametric element is used everywhere except the region connected to the crack front where 15 node pentahedron elements are employed. Along the crack front, a radiating mesh part with 6 layers of equal thickness h is established. A linear finite element modeling is performed to obtain the displacement and stress fields in the plate. The global energy release rate $G(\boldsymbol{\theta}_i)$ corresponding to $\boldsymbol{\theta}_i$ field is then calculated by Eq. (1). This result allows computing the local energy release rate $G(s)$ on the crack front according to Eq. (6). In this section, the crack front is discretized by 30 equally spaced quadratic elements.

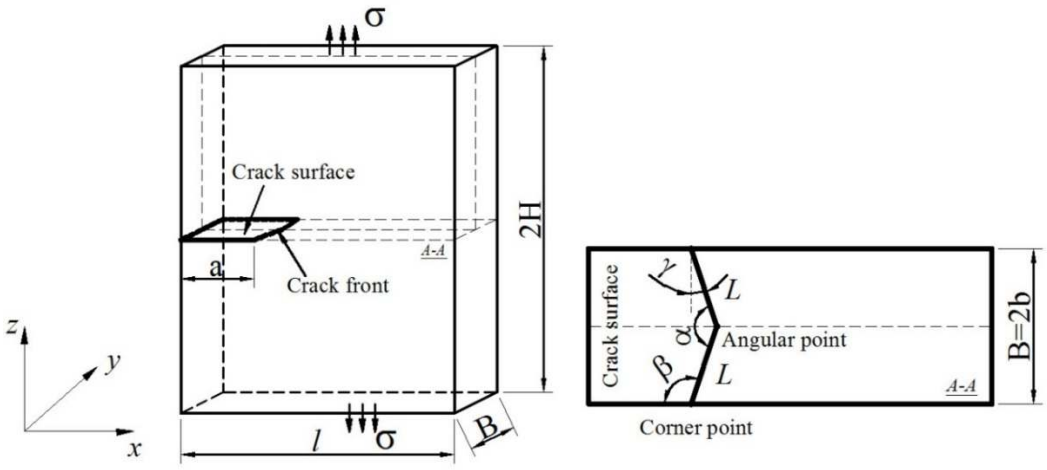

Fig. 5 : Cracked plate under tension.

In order to normalize the energy release rate evaluated by the G-theta method, we use the known result of the stress intensity factor (SIF) in plane strain for a finite plate of width l having a crack of length a submitted to a uniform tension σ (Fig. 7):

$$K_0 = \sigma\sqrt{\pi a}\left(\frac{2b}{\pi a}\tan\frac{\pi a}{2b}\right)^{1/2}\frac{0.752+2.02\frac{a}{b}+0.37\left(1-\sin\frac{\pi a}{2b}\right)^3}{\cos\frac{\pi a}{2b}} \quad (9)$$

and of the energy release rate obtained from Irwin's formula [33]:

$$G_0 = \frac{1-\nu^2}{E}K_0^2 \quad (10)$$

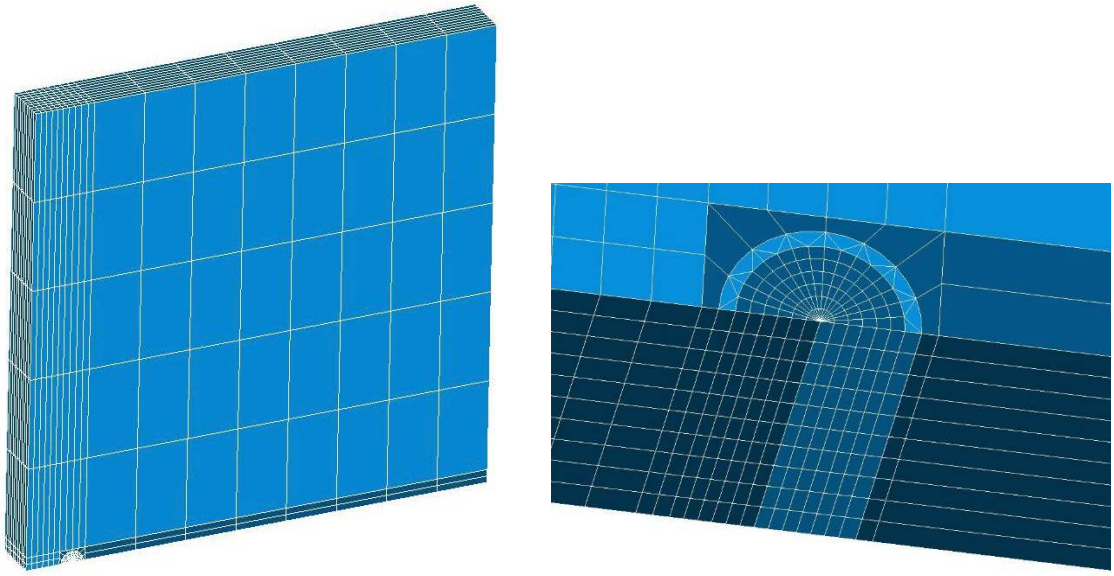

Fig. 6 : Finite element mesh and mesh detail of the crack front.

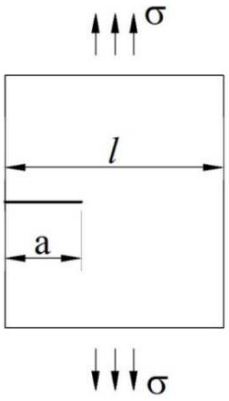

Fig. 7 : Two dimensional cracked plate.

Fig. 9 presents the normalization of the energy release rate G/G_0 calculated along the crack front for different modified lengths L_m of the $\boldsymbol{\theta}$ field. As shown in Fig. 4a, a minimum length $L_{min} = R_{ext}\tan(\gamma)$ is required to ensure $\boldsymbol{\theta}.\boldsymbol{n} = 0$ on the boundary $\partial\Omega$. On the internal portion, the results of G/G_0 are similar for all modified lengths. However, a difference is observed on the boundary layer region L_{min} with an increase of the energy release rate G as the modified length L_m gets larger which stops when $L_m \geq L_{min}$. Moreover, G obtained by G-theta method

with a modified θ field is characterized by an important value at the through point and an almost zero value at the angular point for the case β = 110°. This agrees with the singularity theory developed in the literature [4, 44] and exposed in detail in the next section.

As a matter of fact, the local energy release rate computed by the G-theta method should theoretically be independent of the size of the torus. In practice, the influence of the torus radius is numerically observed for a normal **θ** field and for non-orthogonal crack fronts to free surfaces. As seen in Fig. 10, G corresponding to normal **θ** fields are different in the boundary layer region for two torus sizes with the same $R_{int} = h$ but $R_{ext} = 3h$ and $6h$, respectively. Nevertheless, G calculated by the modified **θ** field is exactly identical for those two cases. Therefore, the modified **θ** field ensures domain integration independence.

The influence of the **θ** field direction was studied recently by Esnault et al. [18] for the stress intensity factors on a simple configuration. The authors have considered a penny-shaped crack in an infinite body loaded in tension and shear. The SIFs were computed by the G-theta method using either a radial **θ** field, normal to the crack front, or a **θ** field tilted by an angle α with respect to that normal. This **θ** field choice allows to avoid the numerical integration of the term A_{ij} in Eq. (7). As a result, no influence of the angle between the normal to the crack front and the **θ** field direction was found in this study. The property is demonstrated generally for non-orthogonal through crack surfaces with the modified **θ** field in this work. Indeed, Fig. 11 shows identical results of local energy release rate along the crack front for different modified **θ** fields. Concretely, a uniform **θ** field parallel to the free surface ($\mathbf{e}_2$) and four modified **θ** fields on four modified lengths $0.2L$, $0.3L$, $0.4L$, $0.5L$ are employed. Therefore, numerical results reproduce well the theory which states that the local energy release rate value $G(s)$ represents the energy necessary to create a virtual crack surface with a unitary value at each calculation point which should be independent of the **θ** field direction.

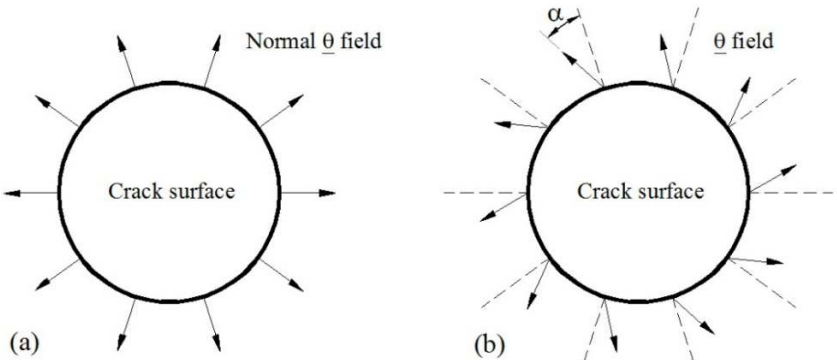

Fig. 8 : **θ** field on the crack front of a penny-shaped crack in an infinite body: (a) normal **θ** field; (b) **θ** field tilted by an angle α with respect to that normal.

The implementation of the modified θ field for non-meshed crack (X-FEM) is quite similar to the case of meshed cracks. The evaluation of stress intensity factors using G-theta method with normal θ field and level sets in Code_Aster has been presented by Geniaut et al. [20]. As observed in Fig. 12, the local energy release rate along the crack front obtained with the modified θ field presents also an improvement in the boundary layer region when compared with a standard normal field in the framework of XFEM. Moreover, the results obtained by FEM and XFEM for the modified θ field are similar.

The advantages of G-theta method with the modified θ field is illustrated in this paper with results obtained for a cracked plate that will be used in the next section to study the corner singularity in a cracked plate. These advantages are also present for more complicated configurations such as part-elliptical cracks in a cylindrical pipe or part-circular cracks in a plate modeled with non-regular mesh which were tested by the authors.

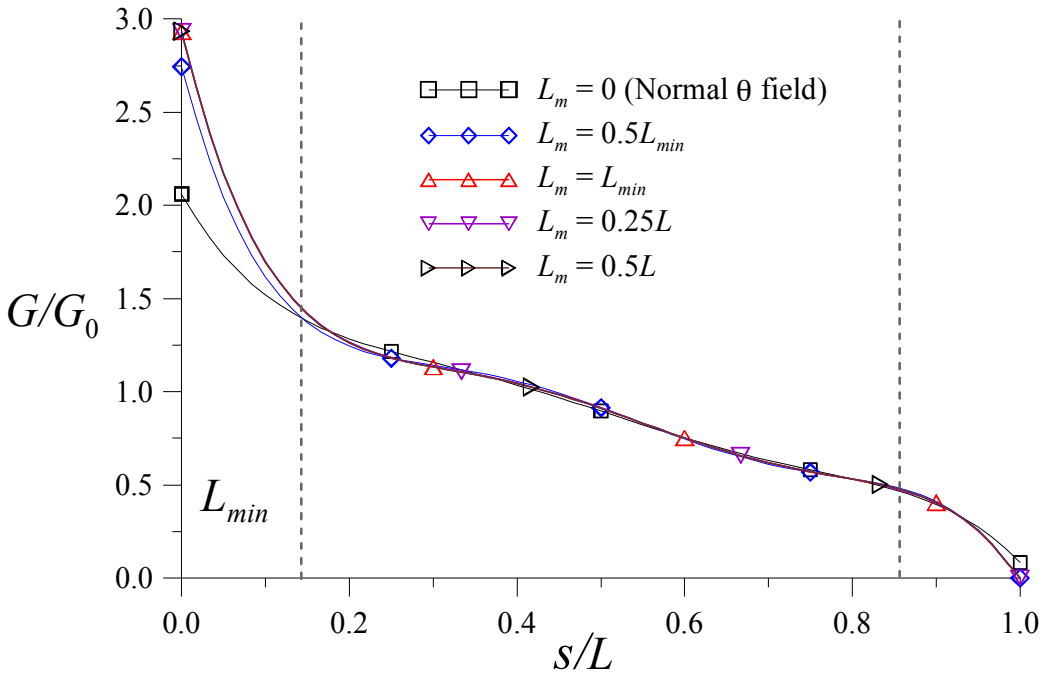

Fig. 9 : Normalized energy release rate along the crack front for different modified lengths L_m of θ field (β=110°).

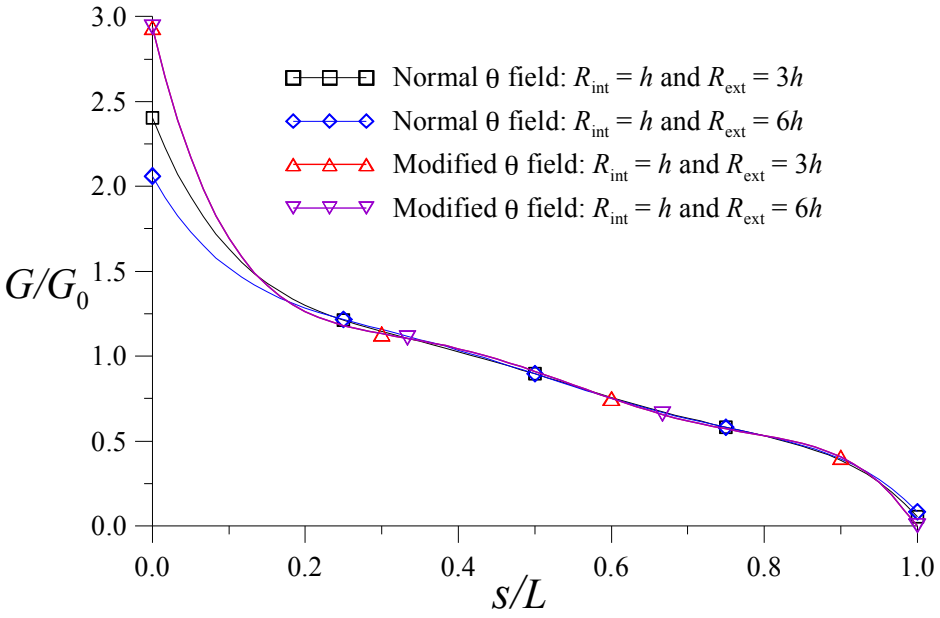

Fig. 10 : Influence of torus size on normalized energy release rate along the crack front (β = 110°).

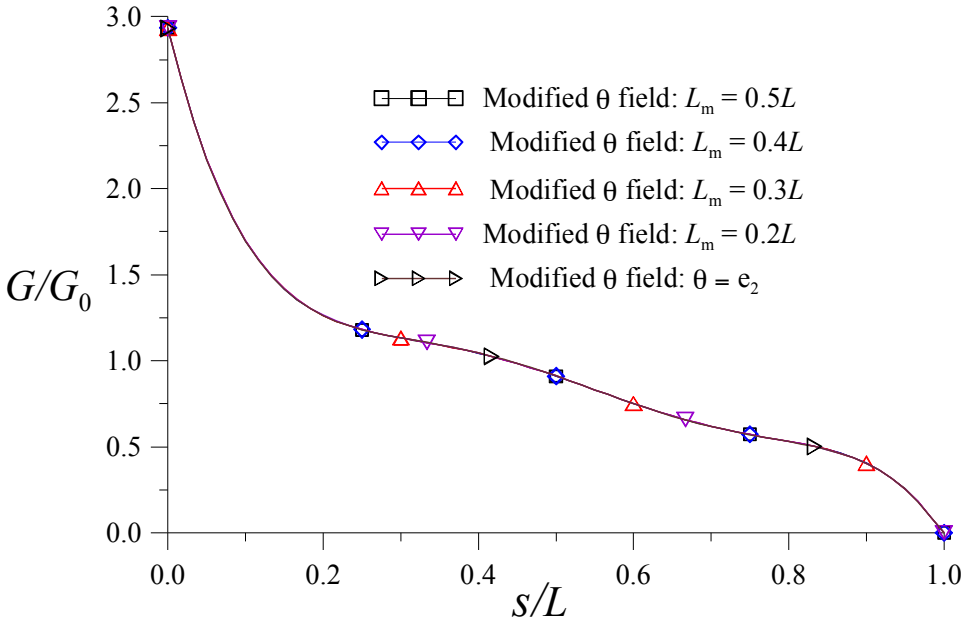

Fig. 11 : Normalized energy release rate along the crack front for different **θ** fields (β=110°).

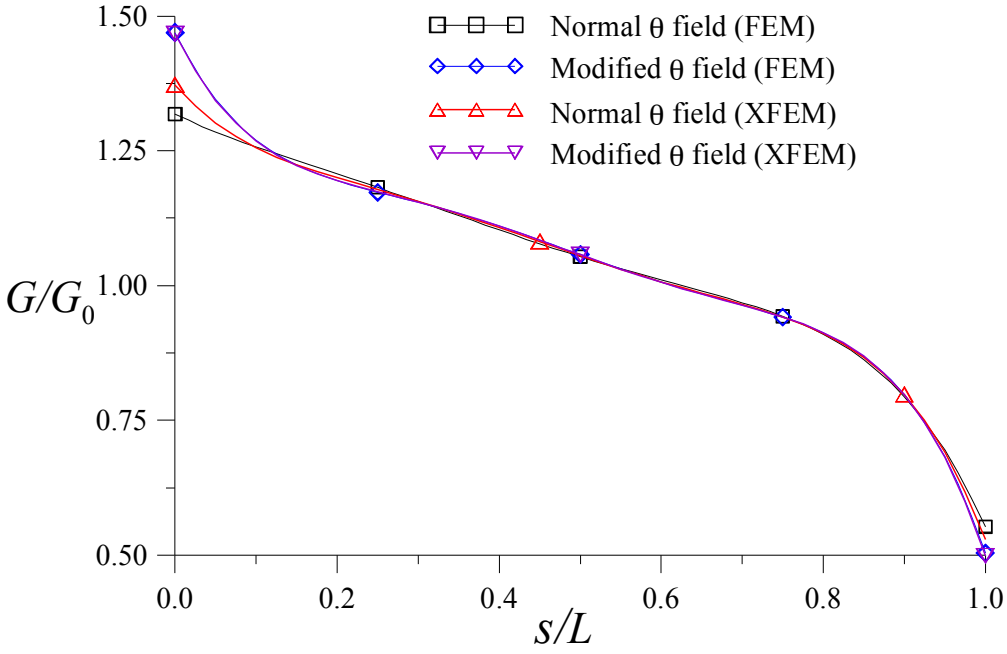

Fig. 12 : Normalized energy release rate computed G by FEM or XFEM for normal or modified θ fields (β=105°).

3 Corner singularities in cracked plates

3.1 Theoretical consideration

Within the tridimensional linear fracture mechanics framework, the well-known square-root stress singularity is valid for smooth parts of crack front [14, 15, 16]. At non-smooth transitions on the crack front and at the intersection of the crack front with a free surface, corner singularity has to be considered. In the vicinity of these points, the displacement fields can be expressed locally in spherical coordinates (Fig. 13) as [5]:

$$\boldsymbol{u} = kR^{\lambda+1}\boldsymbol{g}(\lambda,\phi,\theta) \tag{11}$$

where k is the corner stress intensity factors depending on the external load, λ is the characteristic exponent and $\boldsymbol{g}$ is the angular function only depending on the local geometry and the material properties. The determination of exponent λ at a corner point of a through surface crack is widely investigated as an eigenvalue problem, in which the variational equation governs the displacement distribution on a unit sphere around the singular point. Therefore, the influence of the crack geometry or of the size of the structure (curved crack front, finite body) is not considered in such a method since it is established for a straight crack in a semi-infinite body. However, the local approach using log-log regression analysis for the

stress or the displacement fields can estimate the change of the stress singularity exponent for thin structures [30, 31, 32].

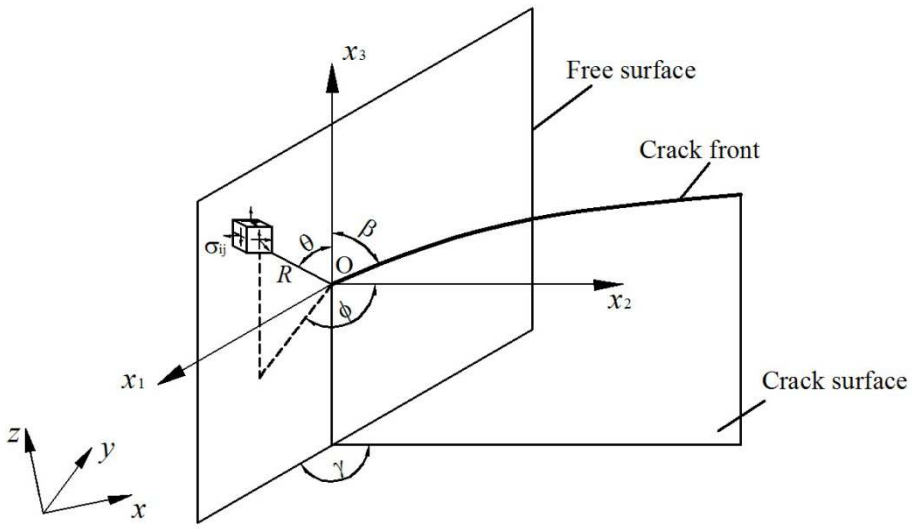

Fig. 13 : Spherical coordinates system with its origin at the terminal point of the crack front at the free surface.

At a point on the crack front sufficiently close to the free surface, the stress field can be expressed either by the classical square-root singularity for an interior point or by the vertex singularity (11). As shown by Benthem [5], the equality of these two equations yields the stress intensity factor $K(s)$ in this layer region as follows:

$$K(s) = ks^{\lambda+\frac{1}{2}} \tag{12}$$

where s is the curvilinear abscissa on the crack front with its origin at the end point on the free surface and k is the corner stress intensity factor. This asymptotic formulation is verified by Nakamura and Parks [41, 42] for an orthogonal crack front.

Besides, Leguillon [36] and Leguillon and Sanchez-Palencia [37] used the matched asymptotic expansions to derive the following expression of the energy release rate within the boundary layer region near the free surface on the crack front:

$$G(s) = Aks^{2\lambda+1} \tag{13}$$

where A is a generic constant depending on the geometry and on the material properties.

Eqs. (12) and (13) present two ways of investigating weak and strong singularities (the Irwin criterion and Griffith one). If $\lambda > -1/2$, the stress intensity factor $K(s)$ and the energy release rate $G(s)$ tend to 0 as s tends to 0 and thus can never reach the critical toughness. Moreover, if $\lambda < -1/2$, $K(s)$ and $G(s)$ tend to infinity and the end point of the crack front undergoes a so-called strong singularity. For a straight crack front orthogonal to the free surface, the well-

known value of λ is -0.4523 > -1/2 corresponding to Poisson's ration ν = 0.3. According to Eqs. (12) and (13), G and K must then be equal to zero at the terminal point of the front edge at the free surface. This result is confirmed theoretically by Shivakumar and Raju [48] and experimentally by Heyer et al. [28]. Those studies in the literature emphasized the fact that the front edge of a crack growth must terminate at the surface obliquely at a certain angle, which ensures a valid square-root stress singularity and the applicability of the classical stress intensity factor concept.

3.2 Numerical investigation for cracked plate

This section is dedicated to studying the influence of plate thickness on corner singularities on the front edge inside a cracked plate as drawn in Fig. 5. The energy release rate along the crack front is calculated by G-theta with a modified θ field to evaluate accurately the value within the boundary layer region near the free surface. The numerical local energy release rate obtained is superposed to the theoretical solution (13) in order to determine the power of the stress singularity λ. Nakamura and Parks [41, 42] showed the numerical solution of stress intensity factor behavior, within the region of 3% of the crack length near the intersection point of an orthogonal front edge with the free surface, which varies accordingly to the formulation (12) for different Poisson's ratio.

The load, material and geometry parameters are defined in the previous section except the plate thickness $2b$, the angle β and Poisson's ratio ν that vary to obtain the corresponding stress singularity exponent λ. The mesh structure is similar to the one shown in Fig. 6 with fifty layers of elements used through the thickness of the plate with increasing thickness from the considered end point of the crack front at the free surface towards the inside of the solid.

The variation of normalized energy release rate G/G_0 along a half-crack front, orthogonal to a free surface, is plotted in Fig. 14 for different Poisson's ratio. The maximum and the minimum values of G/G_0 are located at the points on the centerline and on the free surface, respectively, for non-zero Poisson's ratio. The figure shows that the energy release rate curves decrease considerably in a region sufficiently close to the free surface and that the decrease rate is more pronounced for larger Poisson's ratios. A new plot in log-log scale of the local energy release rate versus the curvilinear abscissa away from the corner point is displayed in Fig. 15. As expected, the profile of G in log-log scale within the boundary layer region is clearly affine. The slope of the curves should correspond to the coefficient $2\lambda+1$ of Eq. (13). It is worth noting that the numerical values λ herein closely agree with the analytical solution of Benthem [5] and the numerical solution derived by eigenvalue problems [4, 6, 14, 21, 22, 49]. Thus, G-theta provides a method to extract the power of stress singularity at a corner point in a cracked plate and to study the influence of plate thickness on this singularity.

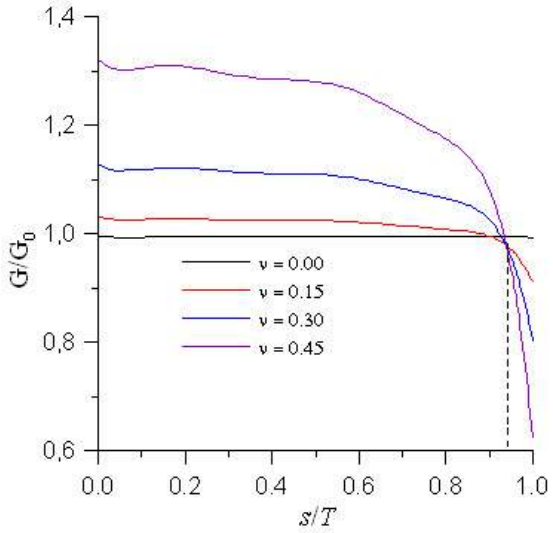

Fig. 14 : Normalized local energy release rate G/G_0 along a half-crack front for various Poisson's ratio ($\beta = 90°$).

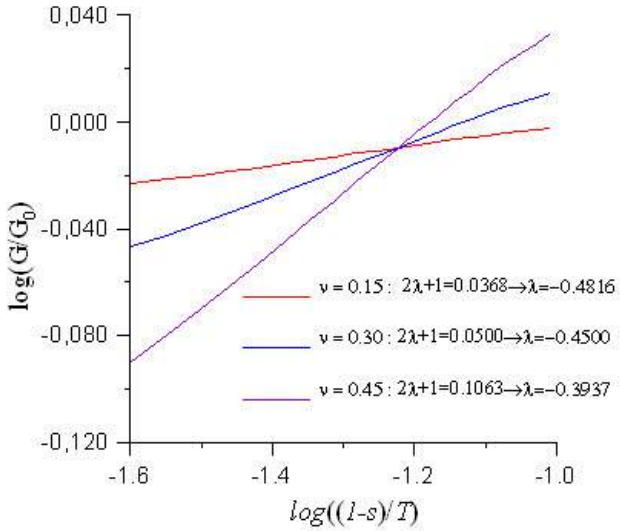

Fig. 15 : Energy release rate profile in the boundary layer region near the free surface ($\beta = 90°$, $b = a$).

For the crack front orthogonal to the free surface, Fig. 16 shows the variation of the stress singularity exponent λ, as a function of Poisson's ratio for different plate thicknesses b. As observed in many others studies, the stress singularity order λ increases with the increase of Poisson's ratio ν. Moreover, the result exhibits that the power λ does not depend on the plate thickness for thick plates ($b \geq 0.1a$) and that its value corresponds to the one obtained by Dimitrov et al. [14]. However, λ increases with the plate thickness b for thin plates ($b < 0.1a$) until the value corresponding to $b = 0.1a$ is reached.

For the crack front non-orthogonal to the free surface, the dependence of the stress singularity order λ versus the crack front angle β is presented in Fig. 16. Using Dimitrov et al. [14] as the reference, we observe that the numerical results match the reference values of an orthogonal

crack front β = 90°. They are higher for β < 90° and lower for β > 90° for all non-zero Poisson's ratio.

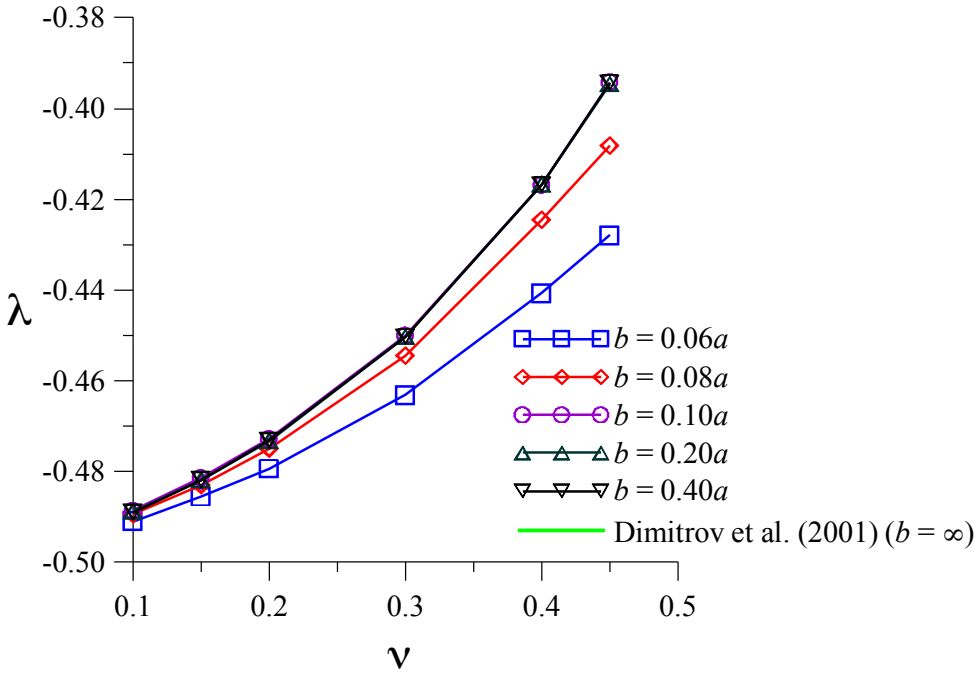

Fig. 16 : Dependence of the stress singularity order λ for the end point at the free surface of the orthogonal crack front with respect to Poisson's coefficient ν for various plate thicknesses *b* (β=90°).

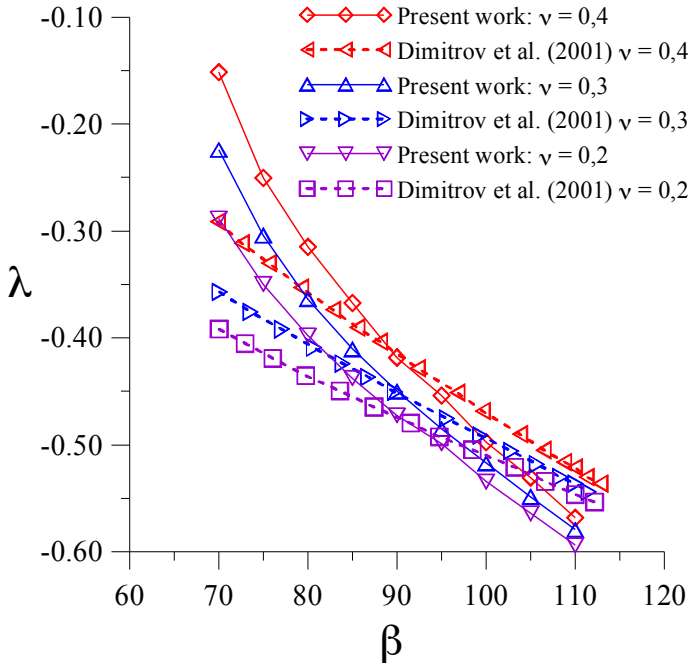

Fig. 17 : Dependence of the singularity order λ at the end point upon the crack front angle β for various Poisson's coefficient ν (*b* = 0.4*a*).

Based on an energy flux argument, Bazant and Estenssoro [4] and Pook [44] suggested that the front edge of a crack under fatigue loading must intersect the free surface at a certain angle β_c to ensure $\lambda = -0.5$. This angle β_c depends upon Poisson's ratio and the inclination of the crack plane. Several experimental results cited by Bui [8] allow checking this phenomenon. Recently, the influence of a 3D corner singularity on fatigue crack growth in transparent specimens of PMMA was investigated experimentally by Herder et al. [28, 29]. Their results show that a practically constant crack front angle was observed and that the process of adjusting this angle occurs continuously. This experimental observation has been verified and confirmed by numerical results. This phenomenon is also noticed by Esnault et al. [18] (Fig. 18). In practice, the front edge can be modified within the boundary layer region, such that $\beta = \beta_c$ in numerical simulation, to enforce the square-root singularity at the terminal point [38]. However, the geometry of the cracked body is not taken into account in the studies mentioned above. Fig. 19 shows the influence of plate thickness on the curve of the critical crack front angle versus Poisson's ratio. Reference results are numerical results obtained by Heyder et al. [28] and empirical results of Pook [44]. As observed, the angle β_c decreases with the decrease of specimen thickness b for a constant Poisson's ratio ν. The limit of β_c is reached as $b \rightarrow \infty$ is obtained by an eigenvalue analysis for a semi-infinite straight crack front [28]. Sevcik et al. [47] used the log-log regression of stress in the vicinity of the crack front for Middle Tension specimen to obtain the angle β_c corresponding to $\lambda = -0.5$. In that work, the change of β_c versus plate thickness is also observed for the thin specimen and its values correspond well with the results of Pook [44] for the thick plate.

The numerical investigation on the 3D corner singularity for the end point of a crack font at the free surface of a cracked plate confirms that the stress singularity exponent λ depends on Poisson's ration ν and on the crack front angle β. However, this shows also the dependence of the power λ and the critical angle β_c upon plate thickness b. Therefore, the results obtained solving an eigenvalue problem with the assumption of a semi-infinite space for the estimation of the vertex singularity should be used with caution for thin plates.

Fig. 18 : Intersection angle of the crack front with the free surface in Mode I fatigue crack growth [18].

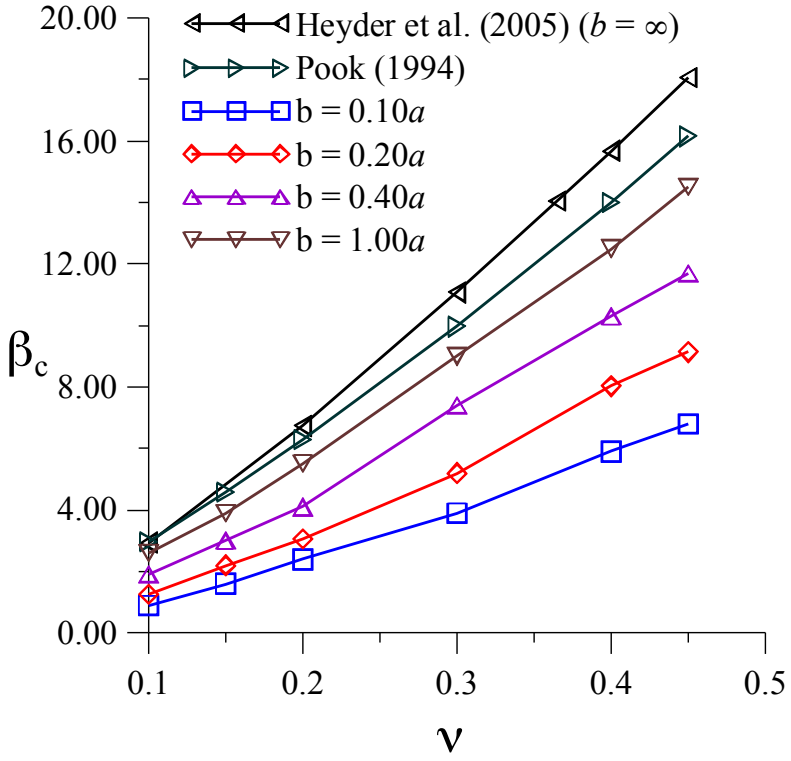

Fig. 19 : Variation of the critical angle between crack front and free surface β_c versus Poisson's coefficient ν for different plate thicknesses *b*.

4 Conclusion

The formulation of the G-theta method and its implementation in the framework of FEM or XFEM for the computation of energy release rate in linear elasticity is described. A modified virtual crack extension (θ field) is proposed to evaluate accurately the energy release rate for the through crack surface with front edge non-orthogonal to the free surface. The modified θ field changes its direction linearly on a certain modified length between the end point, where the θ field is tangent to free surface, and the interior region, where the θ field is normal to the crack front. This modified θ field allows to avoid a brutal change of θ direction between the end point and the nearby adjacent nodes on the non-orthogonal crack front. The numerical results of the energy release rate along the crack front obtained with this modified θ field are independent of the θ field direction and of the torus radius choices. This is not observed numerically for a normal θ field.

The energy release rate along the crack front is then used to evaluate the vertex singularity at the end point of the front edge at the free surface for a cracked plate composed of a singularity exponent and a critical angle. Within the end point region, it is generally only possible to define stress intensity factors and energy release rate in an asymptotic sense. The numerical energy release rate is expressed in logarithmic scale within the boundary layer close to the end point to extract the power of singularity. The critical crack front angle corresponds to the classical square-root stress singularity. For a crack surface perpendicular to the free surface, the stress singularity exponent increases with the increase of Poisson's ratio for a considered intersection angle and decreases with the increase of crack front angle for a considered Poisson's ratio. This tendency corresponds to the one obtained by an eigenvalue problem for a quarter-infinite crack. However, the values of stress singularity exponent are different between these two approaches since this work shows the dependence of vertex singularity to plate thickness. Stress singularity order increases as a function of thickness plate and reaches the value of the eigenvalue problem for the thick plate. The critical crack front angle increases likewise with the increase of plate thickness for a non-zero Poisson's ratio. This numerical investigation on the corner singularity in cracked plates leads us to be careful in using the singularity resulting from the eigenvalue problem for the numerical modeling of crack growth in a finite structure. As this paper considers only straight crack front forms, the influence of the curvature crack front in the boundary layer region close to the end point will be addressed later as well as the case of mixed mode loading.

References

1. Atluri S.N., Nakagaki M., Kathiresan K., Rhee H.C., Chen W.H., Hybrid nite element models for linear and nonlinear fracture analysis. In Proceedings of the International Conference on Numerical Methods in Fracture Mechanics, Luxmore AR, Owen DRJ (eds). Swansea: UK, 1978, 52–66.
2. Barsoum R., On the use of isoparametric finite elements in linear fracture mechanics. International Journal of Numerical Methods in Engineering, 1997, 10: 385-398.
3. Bazant Z.P., Three-dimensional harmonic functions near termination or intersection of gradient singularity line: a general numerical method. International Journal of Engineering Science, 1974, 12: 221–243.
4. Bazant Z.P., Estenssoro L.F., Surface singularity and crack propagation. International Journal of Solids and Structures, 1978, 15: 405–426.
5. Benthem J.P., State of stress at the vertex of a quarter-infinite crack in a half-space. International Journal of Solids and Structures, 1977, 13: 479–492.

6. Benthem J.P., The quarter-infinite crack in a half space; alternative and additional solutions. International Journal of Solids and Structures, 1980, 16: 119-130.
7. Benzley S.E., Representation of singularities with isoparametric nite elements. International Journal for Numerical Methods in Engineering, 1974, 8:537–545.
8. Bui H.D., Fracture Mechanics - Inverse Problems and Solutions. Springer 2006, 382p.
9. Colombo D., Massin P.,Geniaut S., Guiton M., Siavelis M., Tran V.X., Algorithmes de propagation de fissure avec X-FEM. http://www.code-aster.org, Reference documentation R7.02.13, EDF R&D.
10. Colombo D., Massin P., Fast and robust level set update for 3D nonplanar X-FEM crack propagation modelling. Comput. Methods Appl. Mech. Engrg, 2011, 200: 2160-2180.
11. Colombo D., An Implicit Geometrical Approach to Level Sets Update for 3d Non Planar XFem Crack Propagation. Comput. Methods Appl. Mech. Engrg, 2012, 237-240: 39-50.
12. Colombo D., Massin P., Level set propagation for mixed-mode crack advance. European Journal of Computational Mechanics/Revue Européenne de Mécanique Numérique, 2012, 21(3-6) : 1-12.
13. Destuynder Ph., Djaoua M., Lescure S., Quelques remarques sur la mécanique de la rupture elastique. J Méca Théor Appl, 1983, 2 : 113–35.
14. Dimitrov A., Andrä H., Schnack E., Efficient computation of order and mode of corner singularities in 3D-elasticity. International Journal for Numerical Methods in Engineering, 2001, 52: 805–827.
15. Dimitrov A., Andrä H., Schnack E., Singularities near three-dimensional corners in composite. International Journal of Fracture, 2002, 115(4): 361–375.
16. Dimitrov A., Schnack E., Asymptotical expansion in non-Lipschitzian domains - a numerical approach. Numerical Linear Algebra with Applications, 2002, 9: 467–492.
17. EDF R&D: http://www.code-aster.org.
18. Esnault J.B., Doquet V., Massin P., A three-dimensional analysis of fatigue crack paths in thin metallic sheets. International Journal of Fatigue, 2013, http://dx.doi.org/10.1016/j.ijfatigue.2013.03.015.
19. Galenne E., Geniaut S.,Taux de restitution de l'énergie en thermo-élasticité linéaire. http://www.code-aster.org, Reference documentation R7.02.01, EDF R&D.
20. Geniaut S., Massin P., eXtended Finite Element Method. . http://www.code-aster.org, Reference documentation R7.02.12, EDF R&D.

21. Ghahremani F., Numerical variational Method for Extracting 3D Sigularities. International Journal of Solids and Structures, 1991, 27: 1371–1386.
22. Ghahremani F., Shih C.F., Corner singularities of three-dimensional planar interface crack. Journal of Applied Mechanics, 1992, 59: 61–68.
23. Gifford L.N., Hilton P.D., Stress intensity factors by enriched nite elements. Engineering Fracture Mechanics, 1978, 10(3):485–496.
24. Glushkov E., Glushkova N., Lapina O., 3-D elastic stress singularity at polyhedral corner points. International Journal of Solids and Structures, 1999, 36: 1105–1128.
25. González-Albuixech V.F., Giner E., Tarancón J.E., Fuenmayor F.J., Gravouil A., Domain integral formulation for 3-D curved and non-planar cracks with the extended finite element method. Comput. Methods Appl. Mech. Engrg., 2013, 264: 129-144.
26. Gosz M., Dolbow J., Moran B., Domain integral formulation for stress intensity factor computation along curved three-dimensional interface. International Journal of Solids and Structures, 1998, 35: 1763–1783.
27. Gosz M., Moran B., An interaction energy integral method for computation of mixed-mode stress intensity factors along non-planer crack fronts in three dimensions. Engineering Fracture Mechanics, 2002, 69: 299-319.
28. Heyder M., Kolk K., Kuhn G., Numerical and experimental investigations of the influence of corner singularities on 3D fatigue crack propagation. Engineering Fracture Mechanics, 2005, 72: 2095–2105.
29. Heyder M., Kuhn G., 3D fatigue crack propagation: Experimental studies. International Journal of Fatigue, 2006, 28: 627–634.
30. Hutar P., Náhlík L., Knésl Z., The effect of the singularity induced by the free surface on fatigue crack growth in thin structures. Key Eng Mater, 2008, 385–387: 317–20.
31. Hutar P., Náhlík L., Knésl Z., Quantification of the influence of vertex singularities on fatigue crack behavior. Comput Mater Sci, 2009, 45: 653–72.
32. Hutar P, Náhlík L, Knésl Z. The effect of a free surface on fatigue crack behaviour. International Journal of Fatigue, 2010, 32: 1265–69.
33. Irwin G., Analysis of stresses and strains near the end of a crack traversing a plate, Journal of Applied Mechanics, 1957, 24: 361–364.
34. Koguchi H., Stress Singularity Analysis in Three-Dimensional Bonded Structure. International Journal of Solids and Structures, 1997, 34: 461–480.
35. Koguchi H., Muramoto T., The order of stress singularity near the vertex in three-dimensional joints. International Journal of Solids and Structures, 2000, 37: 4737–4762.

36. Leguillon D., Calcul du taux de restitution de l'énergie au voisinage d'une singularité. C.R. Academic Science, Paris 1989, 309 (II) : 945–950.
37. Leguillon D., Sanchez-Palencia E., On 3D cracks intersecting a free surface in laminated composites. International Journal of Fracture, 1999, 99: 25–40.
38. Matos P.F.P., Nowell D., The influence of the Poissons ratio and corner point singularities in three-dimensional plasticity-induced fatigue crack closure: A numerical study. International Journal of Fatigue, 2008, 30: 1930–1943.
39. Mittelstedt C., Becker W., Semi-analytical computation of 3D stress singularities in linear elasticity. Communications in Numerical Methods in Engineering, 2005, 21: 247–257.
40. Mittelstedt C., Becker W., Efficient computation of order and mode of three-dimensional stress singularities in linear elasticity by the boundary finite element method. International Journal of Solids and Structures, 2006, 43: 2868–2903.
41. Nakamura T., Parks D.M., Three-dimensional stress field near the crack front of a thin elastic plate. J. App. Mech, 1988, 55: 805-813.
42. Nakamura T., Parks D.M., Antisymmetrical 3-D stress field near the crack front of a thin elastic plate. Int J Solids Struct, 1989, 25: 1411–20.
43. Pageau S.S., Joseph P.F., Biggers S.B., The order of stress singularities for bonded and disbonded three-material junctions. Int. J. Solids and Struct, 1994, 31: 2979-2997.
44. Pook L.P., Some implications of corner point singularities. Engineering Fracture Mechanics, 1994, 48(3): 367-378.
45. Rice J., Mathematical analysis in the mechanics of fracture. Fracture: an advanced treatise, II, Liebowizt H, Academic Press, 1968.
46. Savruk M.P., Shkarayev S.V., Stress singularities for three-dimensional corners using the boundary integral equation method. Theoretical and Applied Fracture Mechanics, 2001, 36: 263–275.
47. Sevcik M., Hutar P., Zouhar M., Nahlik L., Numerical estimation of the fatigue crack front shape for a specimen with finite thickness. International Journal of Fatigue, 2012, 39: 75–80.
48. Shivakumar K.N., Raju I.S., Treatment of singularities in cracked bodies. International Journal of Fracture, 1990, 45(3): 159–178.
49. Somaratna N., Ting T.C.T., Three-dimensional stress singularities in anisotropic materials and composites. Int. J. Engng Sci., 1986, 24 (7): 1115-1134.
50. Yau J., Wang S., An analysis of interface cracks between dissimilar isotropic materials using conservation integrals in elasticity. Engineering Fracture Mechanics, 1984, 20(3): 423-432.